Steel and Composite Structures, *Vol. 35, No. 6 (2020) 717-727*
DOI: https://doi.org/10.12989/scs.2020.35.6.717

Distortional effect on global buckling and post-buckling behaviour of steel box beams

Noureddine Benmohammed[1], Noureddine Ziane[*1], Sid Ahmed Meftah[1] and Giuseppe Ruta[2]

[1]*Laboratoire des Structures et Matériaux Avancés dans le Génie Civil et Travaux Publics, Université de Djillali Liabes, Sidi Bel Abbes, Algeria*
[2]*Department of Structural & Geotechnical Engineering, University 'La Sapienza', Rome, and National Group for Mathematical Physics, Italy*

(*Received August 3, 2019, Revised May 25, 2020, Accepted May 30, 2020*)

Abstract. The homotopy perturbation method (HPM) to predict the pre- and post-buckling behaviour of simply supported steel beams with rectangular hollow section (RHS) is presented in this paper. The non-linear differential equations solved by HPM derive from a kinematics where large twist and cross-sections distortions are considered. The results (linear and non-linear paths) given by the present HPM are compared to those provided by the Newton–Raphson algorithm with arc length and by the commercial FEM code Abaqus. To investigate the effect of cross-sectional distortion of beams, some numerical examples are presented.

Keywords: post-buckling; homotopy; RHS; distortion; Newton–Raphson

1. Introduction

Due to the advantages involving their high strength-to-weight and stiffness-to-weight ratios, RHS thin-walled beams became very attractive for their use in modern constructions.

Since the theory of thin walled beams was developed by Vlasov (1940) and subsequently refined by Benscoter (1954) for beams with closed cross-sections, the linear behaviour of box beams with rigid cross section has been analysed by several scientists; for sake of space, only a few are quoted here, e.g., Smith and Chopra (1991), Shakourzadeh *et al.* (1995), Kim and White (1997), Loughlan and Ata (1997), Pluzsik and Kollar (2006), Nam-Il Kim (2009). In order to improve the predictability of the model, the assumption of the invariability of the cross-section shape is abandoned in many published works. Among them, Mentrasti (1990) presented a theory of thin-walled beams with deformable rectangular cross-section under torsional and distortional loads, considering the shearing strain in the walls of the beam. In the paper by Suetake and Hirashima (1997) the analytical procedure using extended trigonometric series is reconstructed so that box girders with intermediate diaphragms can be analysed under any end-support and loading conditions. Kim and Kim (1999) developed a method to determine the warping and distortion functions for general thin-walled beams with square cross-sections to carry out some static and free vibration problems. They also extended their theory to thin-walled multicell beams in 2001. Five field variables, including cross-sectional distortion and warping, were consistently employed by Jang *et al.* (2008) to express deformations of straight beams and angled joints. Several numerical problems were solved via finite element formulation and compared with ANSYS results using shell elements. Recently Ren *et al.* (2017) investigated the distortional effect of concentrated eccentric loads on simply supported and cantilever box girders with inner diaphragms using an initial parameter method in which the in-plane shear deformation of diaphragms is fully considered. In spite of the tremendous research activity devoted to the analysis of buckling and lateral-torsional buckling (LTB) of thin walled box beams, most studies were accomplished using the simplifying assumption of non-deformable cross-sections in their own plane (e.g., Vo and Lee 2009, Kim *et al.* 2010, Piovan and Machado 2011, Lanc *et al.* 2015). Among the few available papers on buckling and LTB of thin walled beams with deformable cross-sections, Goncalves and Camotim (2004, 2010), Silvestre and Camotim (2006) and Bebiano *et al.* (2018) have shown that the Generalised Beam Theory (GBT) is a rather powerful tool to assess the local and global buckling behaviour of thin-walled prismatic members. The interactive buckling behaviour of welded steel box-section columns was studied experimentally and numerically by Yang *et al.* (2017). Their experimental results were completed by a parallel finite element simulation. In the same context, Saoula *et al.* (2016) investigated the effect of distortion on the elastic lateral buckling of thin-walled box beams under combined bending and compression. They used Ritz and Galerkin's methods to solve the coupled differential equations. Szymczak and Kujawa (2017) obtained closed-form analytical formulas for the critical stresses for closed square cross-sections with and without internal walls. Recently, Kanishchev and Kvocak (2019) provided a theoretical,

*Corresponding author, Ph.D.
E-mail: zianenoureddine@yahoo.fr

ISSN: 1229-9367 (Print), 1598-6233 (Online)

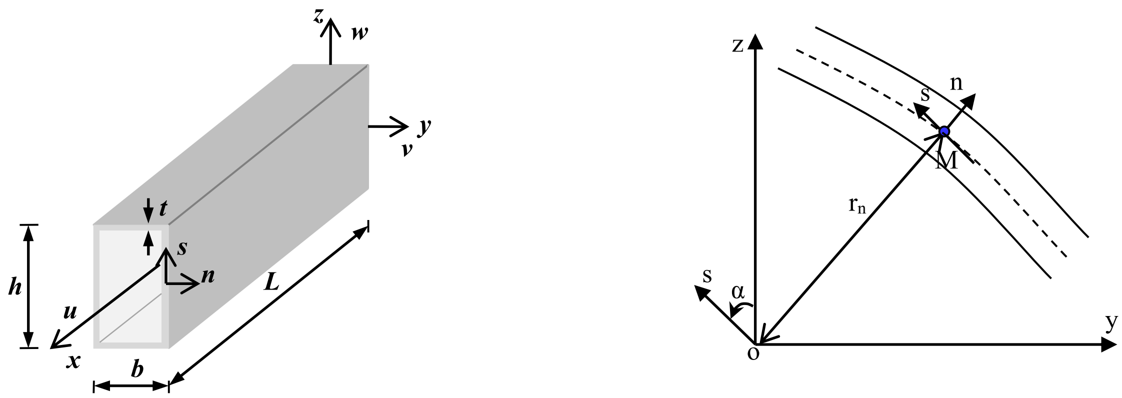

(a) Geometry of a thin-walled RHS beam (b) Coordinate systems

Fig. 1 Geometry of a thin-walled RHS beam and relevant coordinate systems

numerical and experimental analysis of local stability of axially compressed columns made of thin-walled rectangular concrete-filled steel tubes, with the consideration of initial geometric imperfections. They introduced the theory of elastic critical stresses in local buckling of rectangular wall members under uniform compression.

The main objectives of the present paper are: a) to obtain closed-form solutions for the LTB of thin-walled steel RHS beams with distortion; b) to propose an alternative technique based on the homotopy perturbation method (HPM) to analyse the buckling and post-buckling of thin walled rectangular box beams including the deformability of the cross-section; c) to discuss the accuracy of such a method; and d) to discuss the influence of distortion on the critical moment.

2. Theoretical formulation

Consider a thin-walled steel RHS beam of length L, width b, height h and uniform wall thickness t (Fig. 1). The beam is assumed materially and geometrically perfect. Cartesian and curvilinear coordinate systems (x, y, z) and (x, s, n) are related through an angle of orientation α, see Fig. 1 (B). The coordinate s is measured counter-clockwise along the tangent to the middle surface, while n is perpendicular to s. The origin of the Cartesian system is set at the geometrical centre of the cross-section at one end of the beam.

In order to develop the present model, we pose that: a) the beam cross-section is deformable in its own plane; b) the Euler-Bernoulli hypotheses (transverse shear effect related to the bending is neglected) hold; c) to avoid the occurrence of pure local instability , the twist θ of the cross-section can be arbitrarily large, while the distortional displacements are assumed to be small; d) twist and distortion are always coupled.

For non-shearable beams, according to Librescu and Song (2006) and by virtue of the assumption a) above, the displacements, u_x, u_s and u_n of any generic point (M) on the profile section in the x, s and n directions, respectively, may be expressed as

$$\begin{aligned} u_x &= u - y(v' \cos(\theta) + w' \sin(\theta) \\ &\quad - z(v' \sin(\theta) - w' \cos(\theta) - \psi_w \theta' \end{aligned} \tag{1a}$$

$$\begin{aligned} u_s &= -\sin(\alpha)v + \cos(\alpha)w + r_n \sin(\theta) \\ &\quad - s(1-\cos(\theta) + (\psi_{sd} - n\frac{d\psi_{nd}}{ds})\chi \end{aligned} \tag{1b}$$

$$\begin{aligned} u_n &= \cos(\alpha)v + \sin(\alpha)w - (s)\sin(\theta) \\ &\quad - r_n(1-\cos(\theta) + \psi_{nd}\chi \end{aligned} \tag{1c}$$

where u, v, w are the displacements of the centroid (coinciding with the shear centre due to the double symmetry) of the beam cross section in x, y, z directions, respectively, while θ and χ denote the torsion and distortion angle, respectively (see Fig. 2). Primes denote derivatives with respect to the axial abscissa x. According to Sokolnikoff (1946), the warping function ψ_w satisfies the equilibrium and boundary conditions at the cross section outline. It was verified in (Kim and White 1997) that it provides accurate results in static predictions of elastic box beams. Therefore, the same warping function will be used in the current work

$$\psi_w = -yz + \frac{8h^2}{\pi^3}\sum_{j=0}^{\infty}\frac{\sin(\frac{(2j+1)\pi z}{h})\sinh(\frac{(2j+1)\pi y}{h})\sin(\frac{(2j+1)\pi}{2})}{(2j+1)^3\cosh(\frac{(2j+1)\pi b}{2h})} \tag{2a}$$

The distortion of the cross-section is decomposed into rigid-body tangential and normal displacement of each wall. These two addends are provided by the functions ψ_{sd} and ψ_{nd}, respectively, which we find in Kim and Kim (1999) and Jang *et al.* (2008).

$$\psi_{nd} = \begin{cases} \dfrac{4s^3}{(b+h)b} - \dfrac{(2b+h)s}{(b+h)} \ \textit{for the flanges}\ (\alpha = \dfrac{\pi}{2}, \dfrac{3\pi}{2}) \\ -\dfrac{4s^3}{(b+h)h} + \dfrac{(2h+b)s}{(b+h)} \ \textit{for the}\ \text{webs}\ (\alpha = 0, \pi) \end{cases} \tag{2b}$$

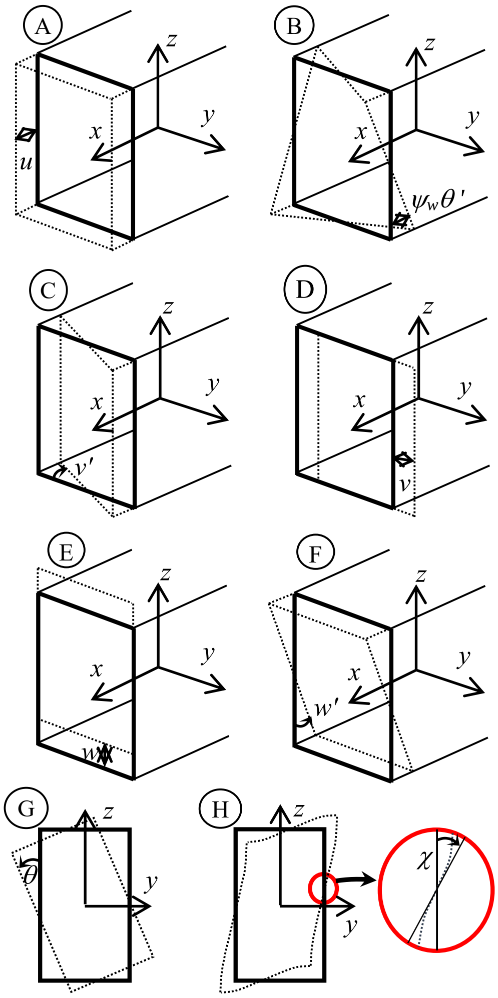

Fig. 2 The Cross-section deformation shapes for : (A) Axial displacement; (B) out-of plane warping; (C) bending rotation about z direction; (D) bending deflection in y direction ; (E) bending deflection in z direction; (F) bending rotation about y direction; (G) torsional rotation; (H) Distortion (in-plane deformation).

$$\psi_{sd} = \frac{bh}{(b+h)}(-1)^{\sin(\alpha)} \quad for\ \alpha = 0, \frac{\pi}{2}, \pi, \frac{3\pi}{2} \tag{2c}$$

Furthermore, the function r_n is defined as

$$r_n = z\sin(\alpha) + y\cos(\alpha) \tag{2d}$$

Recall that the kinematics of Saoula *et al.* (2016) can be obtained by replacing in Eq. (1) the torsion functions *cos*(θ) and *sin*(θ) by 1 and θ, respectively, and disregarding non-linear terms.

In the case of the RHS box beams considered here, we are interested in non-infinitesimal displacements and strains. Hence, strain measures shall be described by the components of Green's strain tensor, which incorporate large displacements

$$\varepsilon_{kl} = \frac{1}{2}\left(\frac{\partial u_k}{\partial x_l} + \frac{\partial u_l}{\partial x_k} + \frac{\partial u_m \partial u_m}{\partial x_k \partial x_l}\right) \tag{3}$$

The adoption of assumptions c) and d), as well as the substitution of Eq. (1) into Eq. (3), lead to the following strain tensor

$$\begin{aligned}\varepsilon_{xx} &= u' - y(v''\cos\theta + w''\sin\theta) \\ &\quad - z(w''\cos\theta - v''\sin\theta) - \psi_w\theta'' \\ &\quad + \frac{1}{2}(v'^2 + w'^2 + (s^2 + r_n^2)\theta'^2)\end{aligned} \tag{4a}$$

$$\gamma_{xs} = (r_n + \frac{d\psi_w}{ds})\theta' + (\psi_{sd} - n\frac{d\psi_{nd}}{ds})\chi' \tag{4b}$$

Since the material constituting the considered RHS beam is supposed to be linear elastic, a generalised form of Hooke's law for the points of the beam walls can be written in the local coordinate system (x,s,n)

$$\sigma_{xx} = E\varepsilon_{xx} \tag{5a}$$

$$\tau_{xs} = G\gamma_{xs} \tag{5b}$$

where (σ_{xx}, τ_{xs}) and (ε_{xx}, γ_{xs}) are the stress and strain components, respectively, while E and G denote Young's and shear moduli, respectively.

4.1 Static balance – Variational formulation

The equilibrium equations can be obtained by using the stationary conditions $\delta(U\text{-}W) = 0$, where U and W are the strain energy and the work spent by the external loads, respectively.

If A denotes the cross-section area, the variation of the strain energy is

$$\delta U = \int_0^L \iint_A \sigma_{xx}\delta\varepsilon_{xx} + \tau_{xs}\delta\gamma_{xs}\, dA dx \tag{6}$$

The variation of the external work for a beam subjected to distributed load with magnitude q_z (see Fig. 3) is defined by

$$\delta W = \int_0^L q_z\delta w + q_z e_y\cos(\theta)\delta\theta - q_z e_z\sin(\theta)\delta\theta dx \tag{7}$$

where e_z, e_y are the eccentricities of the load with respect to the shear centre; the latter is used later as the initial imperfection for the post-buckling analysis.

If the beam is not axially loaded, the equations of equilibrium can be established by using the expressions of the strain energy (Eq. (6)), the work of external loads (Eq. (7)) and the series expansion of cos(θ) and sin(θ), i.e., $1-\theta^2/2$ and θ, respectively. Once integrated by parts, for each arbitrary variation δv, δw, $\delta\theta$ these equations can be written

$$\begin{aligned}&EI_z v'''' + (EI_z - EI_y)(w''''\theta - v''''\theta^2 \\ &+ (2w''' - 4v'''\theta)\theta' + (w'' - 2v''\theta)\theta'') - 2v''\theta'^2) = 0\end{aligned} \tag{8a}$$

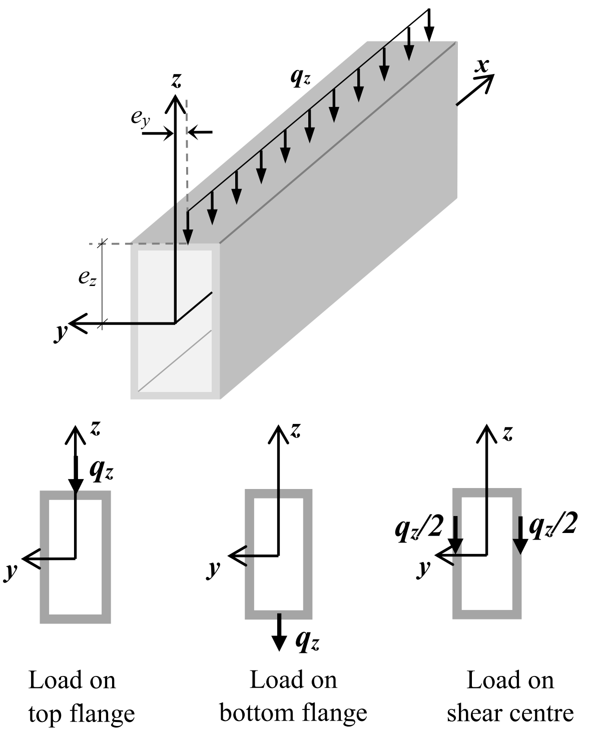

Fig. 3 Thin walled RHS beam under a distributed load q_z with the load height e_z and eccentricity e_y.

$$\begin{aligned}&EI_y w'''' + (EI_z - EI_y)(v''''\theta + w''''\theta^2 \\ &+(2v''' + 4w'''\theta)\theta' + (v'' + 2w''\theta)\theta'') + 2w''\theta'^2) = q_z\end{aligned} \tag{8b}$$

$$\begin{aligned}&EI_w\theta'''' - G(J - \frac{J_{td}^2}{J_d})\theta'' - \frac{3EI_t}{2}\theta'^2\,\theta'' \\ &+(EI_z - EI_y)(w''v'' + (w''^2 - v''^2)\theta) = q_z e_y - q_z e_z\theta\end{aligned} \tag{8c}$$

where the symbols I_y, I_z, I_w, J, I_t, J_d and J_{td} stand for the moments of inertia with respect to the y and z axes, the warping constant, the Saint-Venant torsion constant, the higher order torsion constant, the distortion and the coupled torsion-distortion constants, respectively, defined by

$$I_y = \iint_A z^2 dA \tag{9a}$$

$$I_z = \iint_A y^2 dA \tag{9b}$$

$$I_w = \iint_A \psi_w^2 dA \tag{9c}$$

$$J = \iint_A (r_n - \frac{d\psi_w}{ds})^2 dA \tag{9d}$$

$$I_t = \iint_A (s^2 + r_n^2)^2 dA - \frac{(I_y + I_z)^2}{A} \tag{9e}$$

$$J_d = \iint_A (\psi_{sd} - n\frac{d\psi_{nd}}{ds})^2 dA \tag{9f}$$

$$J_{td} = \iint_A (\psi_{sd} - n\frac{d\psi_{nd}}{ds})(r_n - \frac{d\psi_w}{ds})dA \tag{9g}$$

2.1.1 Lateral-torsional buckling

To establish the expression of the moment inducing lateral buckling with cross-section distortion, Galerkin's method is used for simply supported RHS beams. The displacements are approximated by the means of the following functions, which are compatible with the governing equations and the boundary conditions of the beam

$$\{v, w, \theta\} = \left\{v_{00}\sin(\frac{\pi x}{L}), w_{00}\sin(\frac{\pi x}{L}), \theta_{00}\sin(\frac{\pi x}{L})\right\} \tag{10}$$

where v_0, w_0, θ_0 are the associated displacement amplitudes. Inserting Eq. (10) into Eq. (8b), and carrying out the integration along the beam length at the fundamental state $\{v_{00}, w_{00}, \theta_{00}\} = \{0, w_{00}, 0\}$, we find the linear expression of w_{00} as

$$w_{00} = \frac{5q_z L^4}{384EI_y} \tag{11}$$

where $M_0 = q_z L^2/8$ is the maximum bending moment of the beam under uniform distributed load.

Similarly, the tangent stiffness matrix $[K(M_0, e_z)]$ derived from the algebraic equilibrium equations Eqs. (8) at the fundamental state, is given by

$$K = \begin{bmatrix} \frac{\pi^4 EI_z}{2L^3} & 0 & \frac{5\pi^3 M_0(I_z - I_y)}{36LI_y} \\ 0 & \frac{\pi^4 EI_y}{2L^3} & 0 \\ \frac{5\pi^3 M_0(I_z - I_y)}{36LI_y} & 0 & \frac{25\pi^4 M_0^2 L(I_z - I_y)}{6144EI_y^2} \end{bmatrix} + \begin{bmatrix} 0 & 0 & 0 \\ 0 & 0 & 0 \\ 0 & 0 & \frac{\pi^2 EI_w}{2L^3} - \frac{\pi^2 GJ_{td}^2}{2LJ_d} + \frac{\pi^2 GJ + 8M_0 e_z}{2L} \end{bmatrix} \tag{12}$$

One can obtain the buckling loads by requiring the singularity of the tangent stiffness matrix in Eq. (12), i.e., by imposing $\det([K(M_0, e_z)]) = 0$. This procedure leads to a non-linear algebraic problem for the critical Moments. After some simplifications, the closed-form solutions for the critical LTB moment of simply supported RHS beams under uniformly distributed loading is

$$M_{cr} = \frac{c_1 \pi^2 EI_z}{L^2}\left[c_2 e_z \pm \sqrt{(c_2 e_z)^2 + \frac{I_w}{I_z} + \frac{L^2 G(J - \frac{J_{td}^2}{J_d})}{\pi^2 EI_z}}\right] \quad (13)$$

where the coefficients C_1, C_2 depend on the ratio I_z/I_y in accordance with Mohri *et al.* (2002) and are given by

$$c_1 = \frac{3\pi^4}{256\sqrt{1 - \frac{I_z}{I_y}}} \quad (14a)$$

$$c_2 = \frac{3\pi^2}{64\sqrt{1 - \frac{I_z}{I_y}}} \quad (14b)$$

As it will be seen later, the new expression in Eq. (13) which contains the distortion ratio ($(J_{td})^2/J_d$), reveals that the distortional effect tends to diminish the critical values of the moment.

2.1.2 Linear and non-linear curve

The study of instabilities is not only limited to the determination of bifurcation points, but also extends to post-critical regions. Structural behaviour in these regions is often untreated. This is due to the fact that the governing differential equations in the post-critical region are non-linear and strongly coupled, posing analytical difficulties. The solution of the such non-linear problem is derived via the homotopy perturbation method (HPM) whose expression is

$$\begin{aligned}&(1-p)(EI_z v'''') + p[(EI_z - EI_y)(w''''\theta - v''''\theta^2 \\ &+(2w''' - 4v'''\theta)\theta' + (w'' - 2v''\theta)\theta'') - 2v''\theta'^2) \\ &+EI_z v''''] = 0\end{aligned} \quad (15a)$$

$$\begin{aligned}&(1-p)(EI_y w'''') + p[(EI_z - EI_y)(v''''\theta + w''''\theta^2 \\ &+(2v''' + 4w'''\theta)\theta' + (v'' + 2w''\theta)\theta'') + 2w''\theta'^2) \\ &+EI_y w'''' - q_z] = 0\end{aligned} \quad (15b)$$

$$\begin{aligned}&(1-p)(EI_w\theta'''' - G(J - \frac{J_{td}^2}{J_d})\theta'') \\ &+p[EI_w\theta'''' - G(J - \frac{J_{td}^2}{J_d})\theta'' - \frac{3EI_t}{2}\theta'^2\,\theta'' \\ &+(EI_z - EI_y)(w''v'' + (w''^2 - v''^2)\theta) \\ &-q_z e_y + q_z e_z\theta] = 0\end{aligned} \quad (15c)$$

Where $p \in \{0,1\}$ denote the so-called homotopy parameter. Recall that the linear path is obtained by setting p=0, while for p=1 the path becomes non-linear. Thus, by varying p from 0 to 1, the whole solution is obtained. Note that this method has already been used for other non-linear problems (He 2006, Esmaeilpour and Ganji 2007, Jafarimoghaddam 2019). The solutions of Eq. (15) can be written as a power series in p

$$v = \sum_{i=0}^{m} p^i v_i \quad (16a)$$

$$w = \sum_{i=0}^{m} p^i w_i \quad (16b)$$

$$\theta = \sum_{i=0}^{m} p^i \theta_i \quad (16c)$$

The substitution of Eq. (16) into Eq. (15), followed by the collection of the terms associated with p^i, leads to the following hierarchy of equations:

for p^0

$$EI_z v_0'''' = 0 \quad (17a)$$

$$EI_y w_0'''' - q_z = 0 \quad (17b)$$

$$EI_w\theta_0'''' - G(J - \frac{J_{td}^2}{J_d})\theta_0'' - q_z e_y = 0 \quad (17c)$$

for p^1

$$\begin{aligned}&EI_z v_1'''' + (EI_z - EI_y)(w_0''''\theta_0 - v_0''''\theta_0^2 \\ &+(2w_0''' - 4v_0'''\theta_0)\theta_0' + (w_0'' - 2v_0''\theta_0)\theta_0'') - 2v_0''\theta_0'^2) = 0\end{aligned} \quad (17d)$$

$$\begin{aligned}&EI_z w_1'''' + (EI_z - EI_y)(v_0''''\theta_0 + w_0''''\theta_0^2 \\ &+(2v_0''' + 4w_0'''\theta_0)\theta_0' + (v_0'' + 2w_0''\theta_0)\theta_0'') + 2w_0''\theta_0'^2) = 0\end{aligned} \quad (17e)$$

$$\begin{aligned}&EI_w\theta_1'''' - G(J - \frac{J_{td}^2}{J_d})\theta_0'' - \frac{3EI_t}{2}\theta_0'^2\theta_0'' \\ &+(EI_z - EI_y)(w_0''v_0'' + (w_0''^2 - v_0''^2)\theta_0) + q_z e_z\theta_0 = 0\end{aligned} \quad (17f)$$

For sake of space, the terms associated with the coefficients p^i when $i \geq 2$, can not be displayed here.

Moreover, the boundary conditions for simply supported RHS beam are given by

$$\begin{cases} v_i(0) = 0 \\ v_i''(0) = 0 \\ v_i(L) = 0 \\ v_i''(L) = 0 \end{cases} \quad (18a)$$

$$\begin{cases} w_i(0) = 0 \\ w_i''(0) = 0 \\ w_i(L) = 0 \\ w_i''(L) = 0 \end{cases} \quad (18b)$$

Table 1 Buckling moments (kN.m) when the load is applied on top flange, e_z = 0.3 m

L (m)	t (cm)	Present Eq. (13)	Saoula et al. (2016) with Galerkin	Saoula et al. (2016) with Ritz	Saoula et al. (2016) with FEM	GBT	Δ1	Δ2	Δ3	Δ4
10.00	2.00	16133.45	16109.14	15855.04	15868.75	16076.17	0%	2%	2%	0.3%
	2.50	20210.51	20145.86	19829.85	21157.50	21435.71	0%	2%	5%	6%
12.00	2.00	13572.16	13675.56	13448.83	14079.78	14209.69	1%	1%	4%	4%
	2.50	17002.25	17102.33	16820.31	18484.20	18656.19	1%	1%	9%	9%

Table 2 Buckling moments (kN.m) when the load is applied on centroid, e_z = 0.0 m

L (m)	t (cm)	Present Eq. (13)	Saoula *et al.* (2016) with Galerkin	Saoula *et al.* (2016) with Ritz	Saoula *et al.* (2016) with FEM	GBT	Δ1	Δ2	Δ3	Δ4
10.00	2.00	17174.40	16092.94	15794.60	16622.40	16834.61	7%	9%	3%	2%
	2.50	21516.69	22592.56	22104.00	22130.00	22405.16	5%	3%	3%	4%
12.00	2.00	14298.90	13675.56	15197.84	14618.88	14746.92	5%	6%	2%	3%
	2.50	17914.17	18819.58	18413.98	19177.20	19343.10	5%	3%	7%	7%

Table 3 Buckling moments (kN.m) when the load is applied on bottom flange, e_z = -0.3 m

L (m)	t (cm)	Present Eq. (13)	Saoula *et al.* (2016) with Galerkin	Saoula *et al.* (2016) with Ritz	Saoula *et al.* (2016) with FEM	GBT	Δ1	Δ2	Δ3	Δ4
10.00	2.00	18282.52	17822.27	17364.15	17371.25	17618.27	3%	5%	5%	3%
	2.50	22907.28	23742.27	23082.38	23078.75	23402.67	4%	1%	1%	2%
12.00	2.00	15064.56	15530.69	15968.73	15147.36	15295.45	3%	6%	1%	1%
	2.50	18875.01	20726.52	20147.24	19848.6	20043.62	9%	7%	5%	6%

$$\begin{cases} \theta_i(0)=0 \\ \theta_i''(0)=0 \\ \theta_i(L)=0 \\ \theta_i''(L)=0 \end{cases} \tag{18c}$$

In order to solve the non-linear problem in Eq. (17), the initial linear solutions v_0, w_0, θ_0 can easily be obtained after replacing the general solutions of Eqs. (17(a)-17(c)) in the boundary conditions Eq. (18). Once these solutions $v_0(q_z)$, $w_0(q_z)$, $\theta_0(q_z)$ are replaced into Eqs. (17(d)-17(f)) we obtain $v_1(q_z)$, $w_1(q_z)$, $\theta_1(q_z)$. Thus, the solutions for $i \geq 2$ are obtained by following the same procedure.

To validate the accuracy of the HPM, the non-linear equation given in Eq. (8) are solved by the help of the classical iterative Newton–Raphson method with arc length. The expressions of the tangent stiffness symmetric matrix coefficients *Kij* may be found in Appendix.

3. Results and discussion

3.1 Lateral torsional buckling moment with distortion

In order to validate the closed-form solutions presented earlier, the present values of the buckling moments obtained by Eq. (13) are compared with those obtained by Saoula et al. (2016) and by Generalised Beam Theory (GBT). For this purpose, a simply supported steel beam with rectangular hollow section is considered. In this comparative study we take E=210 Gpa, G=80.77 Gpa, h=0.6 m and b=0.2 m, while the beam length L and wall thickness t are variable (see Tables 1-3). The GBT results are obtained by means of the GBTUL 2.0 code, in which the RHS beams are discretized longitudinally into 10 elements and transversally into 4 natural nodes, 3 intermediate nodes for each flange and 5 intermediate nodes for each web. As it is well-known, buckling of short beams occurs in local mode. Therefore, by virtue of the assumption c), the beams with length L<10 m are abandoned in this study.

It can be seen from the comparison shown in Tables 1-3 that the present results agree well with those obtained by Saoula *et al.* (2016) and GBT. The relative error is

$$\Delta 1 = \frac{|(present\ M_{cr}) - (Saoula\ et\ al.\ with\ Galerkin)|}{Min(present\ M_{cr}, Saoula\ et\ al.\ with\ Galerkin)} \quad (19a)$$

$$\Delta 2 = \frac{|(present\ M_{cr}) - (Saoula\ et\ al.\ with\ Ritz)|}{Min(present\ M_{cr}, Saoula\ et\ al.\ with\ Ritz)} \quad (19b)$$

$$\Delta 3 = \frac{|(present\ M_{cr}) - (Saoula\ et\ al.\ with\ FEM)|}{Min(present\ M_{cr}, Saoula\ et\ al.\ with\ FEM)} \quad (19c)$$

$$\Delta 4 = \frac{|(present\ M_{cr}) - GBT)|}{Min(present\ M_{cr}, GBT)} \quad (19d)$$

3.2 Pre- and post- buckling results

The purpose of this section is to compare the equilibrium paths provided by the HPM, Newton-Raphson and FEM. The effect of distortion on the non-linear solution is also discussed. In all computations, the initial imperfection e_y is assumed to be 10^{-4} m. We use a RHS steel beam with L=12 m, b=0.2 m, h=0.6 m, t=0.02 m. Three load positions are considered, i.e., the load can be applied to the top flange, bottom flange or on the shear centre.

The non-linear problem in Eq. (8) is solved by the HPM, which requires power series of 80 terms (m=80 in Eq. (16)). The same problem is solved by Newton-Raphson method for which arc-length can be held constant (equal to unity) or reduced if convergence fails; the maximum tolerance is 10^{-6}. The finite element simulation is carried out by using Abaqus software with two element types. The first type of element (S8R) is restricted to RHS beam considering distortion, while the second (B32) is adopted to mesh non-deformable cross-section beams.

In the case of RHS beam with distortion Figs. 4-9 show that the linear paths as well as the bifurcation points found by the HPM are quite close to those obtained by Newton-Raphson method and shell finite element analysis (S8R); the maximum relative error is 3%. This error remains acceptable for all non-linear paths (q_z, w_{00}), (q_z, v_{00}), (q_z, θ_{00}) when the load is applied on the top flange. These figures also reveal that for the post-buckling equilibrium paths (q_z, w_{00}) and (q_z, θ_{00}) of the beams loaded at bottom flange and shear centre there are only small discrepancies among the three models results. For the non-linear curves (q_z, w_{00}), the difference between the three models becomes more and more important as one moves away from the critical region. Note that the FEM with shell element provides only short post-buckling paths. This is due to the fact that the local buckling occurs near the overall bifurcation point; a similar remark can be found in Ed-dinari *et al.* (2014) for open section beams.

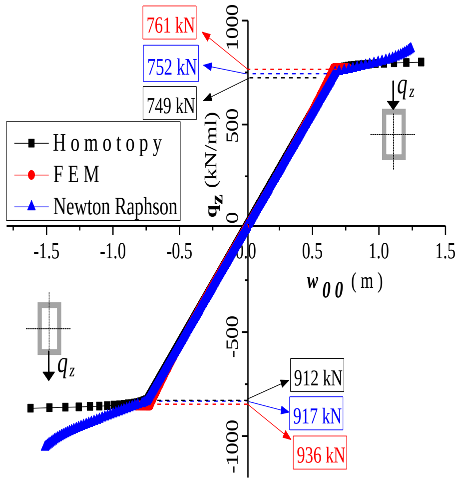

Fig. 4 Pre and post-buckling equilibrium paths (q_z, w_{00}) with distortional effect. Load on top flange (top-right curve).Load on bottom flange (bottom-left curve)

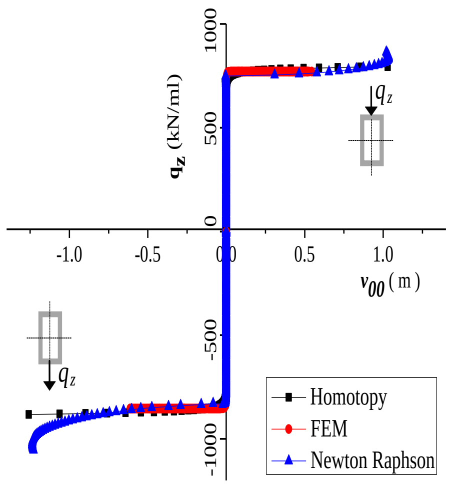

Fig. 5 Pre and post-buckling equilibrium paths (q_z, v_{00}) with distortional effect. Load on top flange (top-right curve). Load on bottom flange (bottom-left curve)

From Figs. 7-9 it can be seen that the buckling load provided by FEM with beam element (B32) is slightly lower than those predicted by the HPM and Newton-Raphson method (the maximum relative error is of order 6%). These plots also show that models without distortion overestimate the buckling load as compared to models with distortion; the difference between the predictions obtained via the two approach (HPM with and without distortion) can reach 32%.

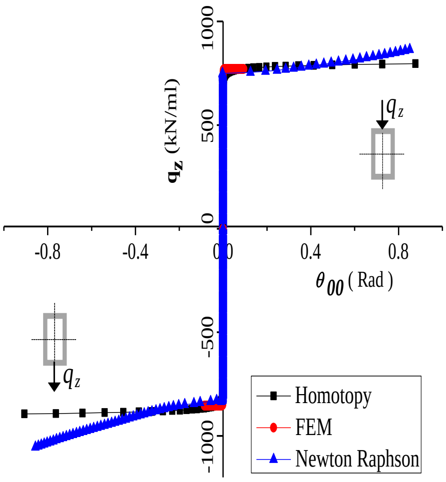

Fig. 6 Pre and post-buckling equilibrium paths (q_z, θ_{00}) with distortional effect. Load on top flange (top-rightcurve). Load on bottom flange (bottom-left curve)

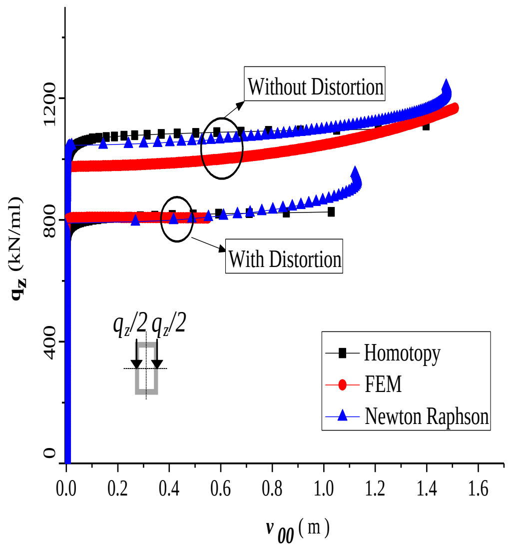

Fig. 8 Pre and post-buckling equilibrium paths (q_z, v_{00}) with and without distortional effect. Load on the shear centre

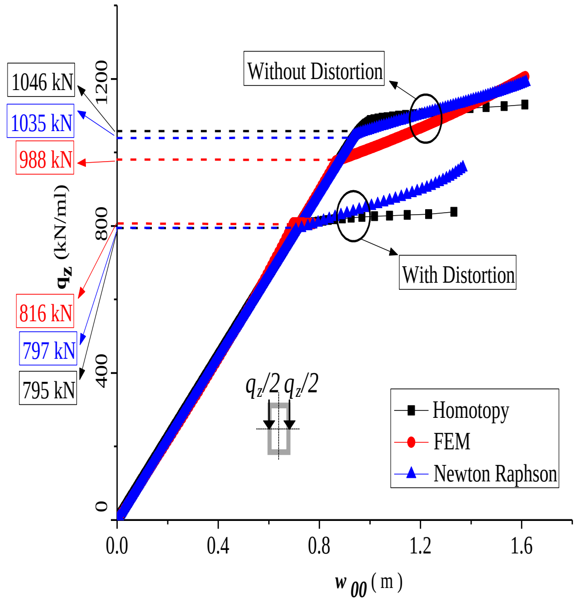

Fig. 7 Pre and post-buckling equilibrium paths (q_z, w_{00}) with and without distortional effect. Load on the shear centre

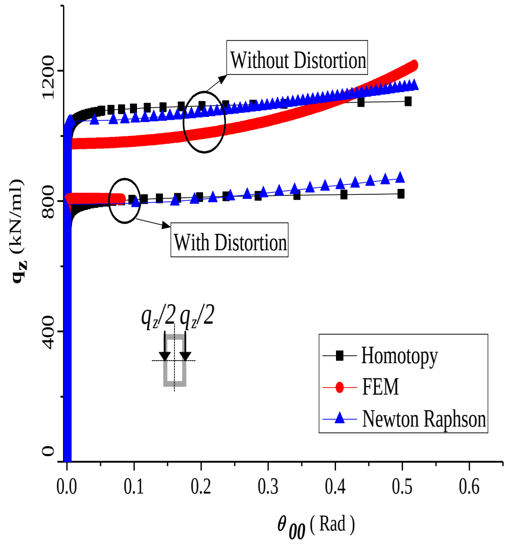

Fig. 9 Pre and post-buckling equilibrium paths (q_z, θ_{00}) with and without distortional effect. Load on the shear centre

4. Conclusions

To highlight the influence of distortion on the lateral-torsional buckling and post-buckling behaviour of simply supported RHS steel beams, we have proposed on the one hand a new closed form solution to predict buckling loads and, on the other hand, three methods (HPM, Newton Raphson and FEM) to obtain the pre- and post-buckling equilibrium paths. The non-linear equilibrium equations have been established by using large displacements, large twist angles and small distortion angles. The main results are:

- The present buckling loads obtained by Eq. (13) agree well with those in Saoula *et al.* (2016) and with the results obtained by GBTul code.

- Linear paths and bifurcation points computed by the HPM coincide exactly with those provided by Newton Raphson method and FEM.
- Contrary to the non-linear curves (q_z,w_{00}) for e_z=0, e_z=-0.3, showing remarkable differences between the three approaches, the other curves exhibit similar post-buckling behaviour.
- The present model with distortion underestimates the buckling load as compared to that of the classical models without distortional. This means that the present model is conservative.

Acknowledgments

We acknowledge the support of institutional grants of the Algerian Directorate General for Scientific Research and Technological Development. Thanks are also due to "La Sapienza" University, Rome, Italy, for the cooperation.

References

Abaqus Standard User's Manual, Version 6.4. (2003), Hibbit, Karlsson and Sorensen Inc., Pawtucket, RI, USA.

Bebiano, R., Basaglia, C., Camotim, E. and Gonçalves, R. (2018), "GBT buckling analysis of generally loaded thin-walled members with arbitrary flat-walled cross-sections", *Thin-Wall. Struct*., **123**, 11-24. https://doi.org/10.1016/j.tws.2017.10.04.

Benscoter, S.U. (1954), "A theory of torsion bending for multicell beams", *J. Appl. Mech*., **20**, 25-34.

Ed-dinari A., Mottaqui, H., Braikat, B., Jamal, M., Mohri, F. and Damil, N. (2014), "Large torsion analysis of thin-walled open sections beams by the Asymptotic Numerical Method", *Eng. Struct*., **81**, 240-255. https://doi.org/10.1016/j.engstruct.2014.09.045.

Esmaeilpour, M. And Ganji, D.D. (2007), "Application of He's homotopy perturbation method to boundary layer flow and convection heat transfer over a flat plate", *Phys. Lett. A*, **372**(1), 33-38. https://doi.org/10.1016/j.physleta.2007.07.002.

Ferrarotti, A., Ranzi, G., Taig, G. and Piccardo, G. (2017), "Partial interaction analysis of multi-component members within the GBT", *Steel Compos. Struct*., **25**(5), 625-638. https://doi.org/10.12989/scs.2017.25.5.625.

GBTUL, Version 2.0.4.3 (2013), The Generalised Beam Theory Research Group, Instituto superior Técnico, Lisbon, Portugal.

Gonçalves, R. and Camotim, D. (2004), "Buckling analysis of single and multi-cell closed thin-walled metal members using Generalised Beam Theory", *Proceedings of the 4th International Conference On Coupled Instabilities In Metal Structures*, Rome, 27–29/9.

Gonçalves, R. and Camotim, D. (2010), "Steel-concrete composite bridge analysis using generalised beam theory", *Steel Compos. Struct*., **10**(3), 223-243. https://doi.org/10.12989/scs.2010.10.3.223.

He, J.H. (2006), "Homotopy perturbation method for solving boundary value problems", *Phys. Lett. A*, **350**, 87-88. https://doi.org/10.1016/j.physleta.2005.10.005.

Jafarimoghaddam, A.(2019), "On the Homotopy Analysis Method (HAM) and Homotopy Perturbation Method (HPM) for a nonlinearly stretching sheet flow of Eyring-Powell fluids", *Eng. Sci. Technol. Int. J.*, **22**(2), 439-451. https://doi.org/10.1016/j.jestch.2018.11.001.

Jang, G.W., Kim, K.J. and Kim, Y.Y. (2008), "Higher-order beam analysis of box beams connected at angled joints subject to out-of-plane bending and torsion", *Int. J. Numer. Method. Eng.*, **75**(11), 1361-1384. https://doi.org/10.1002/nme.2314

.Kanishchev, R. and Kvocak, V. (2019), "Local buckling of rectangular steel tubes filled with concrete", *Steel Compos. Struct.*, **31**(2), 201-216.

Kim, C. and White, S.R. (1997), "Thick-walled composite beam theory including 3-d elastic effects and torsional warping", *lnt. J. Solids Struct.*, **34**, 4237-4259. https://doi.org/10.1016/S0020-7683(96)00072-8.

Kim, J.H. and Kim, Y.Y. (1999), "Analysis of thin-walled closed beams with general quadrilateral cross sections", *J. Appl. Mech*., **66**, 904-912. https://doi.org/10.1115/1.2791796.

Kim, J. H. and Kim, Y.Y. (2001), "Thin-walled multicell beam analysis for coupled torsion, distortion, and warping deformations", *J. Appl. Mech.*, **68**, 260-269. https://doi.org/10.1115/1.1357166.

Kim N.I. (2009), "Dynamic stiffness matrix of composite box beams", *Steel Compos. Struct.*, **9**(5), 473-497. https://doi.org/10.12989/scs.2009.9.5.473.

Kim N.I., Shin, D.K. and Park, Y.S. (2010), "Coupled stability analysis of thin-walled composite beams with closed cross-section", *Thin-Wall. Struct.*, **48**(8), 581-596. https://doi.org/10.1016/j.tws.2010.03.006.

Lanc, D. Vo, T.P., Turkalj, G. and Lee, J. (2015), "Buckling analysis of thin-walled functionally graded sandwich box beams", *Thin-Wall. Struct.*, **86**, 148-156. https://doi.org/10.1016/j.tws.2014.10.006.

Librescu, L. and Song, O. (2006), *Thin-Walled Composite Beams Theory and Application*, Springer, Dordrecht, Netherlands.

Loughlan, J. and Ata, M. (1997), "The behaviour of open and closed section carbon fibre composite beams subjected to constrained torsion", *Compos. Struct*., **38**(1-4), 631-647. https://doi.org/10.1016/S0263-8223(97)00101-3.

Mentrasti, L. (1990), "Distortion (and Torsion) of rectangular thin-walled beams", *Thin- Wall. Struct*., **10**(3), 175-193. https://doi.org/10.1016/0263-8231(90)90062-4.

Mohri, F., Azrar, L. and Potier-Ferry, M. (2002), "Lateral post-buckling analysis of thin-walled open section beams", *Thin-Wall. Struct*., **40**(12), 1013-1036. https://doi.org/10.1016/S0263-8231(02)00043-5.

Piovan, M.T. and Machado, S.P. (2011), "Thermo elastic dynamic stability of thin-walled beams with graded material properties", *Thin-Wall. Struct*., **49**(3), 437-447. https://doi.org/10.1016/j.tws.2010.11.002.

Pluzsik, A. and Kollàr, L.P. (2006), "Torsion of closed section, orthotropic, thin-walled beams", *Int. J. Solids Struct*., **43**(17), 5307-5336. https://doi.org/10.1016/j.ijsolstr.2005.08.001.

Ren, Y., Cheng, W., Wang, Y. and Wang, B. (2017), "Analysis of the distortion of cantilever box girder with inner flexible diaphragms using initial parameter method", *Thin-Wall. Struct*., **117**, 140-154. https://doi.org/10.1016/j.tws.2017.04.010.

Ren, Y., Cheng, W., Wang, Y., Chen, Q. and Wang, B. (2017), "Distortional analysis of simply supported box girders with inner diaphragms considering shear deformation of diaphragms using initial parameter method", *Eng. Struct*., **145**, 44-59. https://doi.org/10.1016/j.engstruct.2017.05.004.

Saoula, A., Meftah, S.A., Mohri, F. and Daya, E.M. (2016), "Lateral buckling of box beam elements under combined axial and bending loads", *J. Constr. Steel Res*., **116**, 141-155. https://doi.org/10.1016/j.jcsr.2015.09.009.

Shakourzadeh, H., Guo, Y.Q. and Batoz, J.L. (1995), "A torsion bending element for thin-walled beams with open and closed cross sections", *Comput. Struct*., **55**(6), 1045-1054. https://doi.org/10.1016/0045-7949(94)00509-2.

Silvestre, N. and Camotim, D. (2006), "Vibration behaviour of

axially compressed cold-formed steel members", *Steel Compos. Struct.*, **6**(3), 221-236. https://doi.org/10.12989/scs.2006.6.3.221.
Smith, E.C. and Chopra, I. (1991), "Formulation and evaluation of an analytical model for composite box-beams", *J. Am. Helicopt. Soc.*, **36**(3), 23-35. https://doi.org/10.4050/JAHS.36.23.
Sokolnikoff, I.S. (1946), *Mathematical Theory of Elasticity*, McGraw-Hill, New York, USA.
Suetake, Y. and Hirashima, M. (1997), "Extended trigonometric series analysis of box girders with diaphragms", *J. Eng. Mech.*, **123**(4), 293-301. https://doi.org/10.1061/(ASCE)0733-9399(1997)123:4(293).
Szymczak, C. and Kujawa, M. (2017), "Distortional buckling of thin-walled columns of closed quadratic cross-section", *Thin-Wall. Struct.*, **113**, 111-121. https://doi.org/10.1016/j.tws.2017.01.006.
Vlasov, V.Z. (1940), *Thin Walled Elastic Beams*. Russian original book; Stroizdat, Moscow, French translation (1962): *Pieces Longues En Voiles Minces*, Eyrolles, Paris, France.
Vo, T.P. and Lee, J. (2009), "Free vibration of axially loaded thin-walled composite box beams", *Compos. Struct.*, **90**(2), 233-241. https://doi.org/10.1016/j.compstruct.2009.03.010.
Yang, L., Shi, G., Zhao, M. and Zhou, W. (2017), "Research on interactive buckling behavior of welded steel box-section columns", *Thin-Wall. Struct.*, **115**, 34-47. https://doi.org/10.1016/j.tws.2017.01.030.

CC

Appendix

$$K_{11} = \frac{E\pi^4(4I_z - 3\theta_{00}^2(I_z - I_y))}{8L^3} \tag{A.1}$$

$$K_{12} = \frac{4E\pi^3\theta_{00}(I_z - I_y)}{3L^3} \tag{A.2}$$

$$K_{13} = \frac{E\pi^3(16w_{00} - 9v_{00}\theta_{00}\pi(I_z - I_y))}{12L^3} \tag{A.3}$$

$$K_{22} = \frac{E\pi^4(4I_y + 3\theta_{00}^2(I_z - I_y))}{8L^3} \tag{A.4}$$

$$K_{23} = \frac{E\pi^3(16v_{00} + 9w_{00}\theta_{00}\pi(I_z - I_y))}{12L^3} \tag{A.5}$$

$$\begin{aligned} K_{33} = {} & \frac{6E\pi^4(w_{00}^2 - v_{00}^2)(I_z - I_y)}{16L^3} \\ & + \frac{8q_z L^4 e_z + 8EI_w\pi^4 + 9EI_t\pi^4\theta_{00}^2 + 8\pi^2 GJL^2}{16L^3} \\ & - \frac{\pi^2 GJJ_{td}^2}{2LJ_d} \end{aligned} \tag{A.6}$$

$$K_{21} = K_{12} \tag{A.7}$$

$$K_{31} = K_{13} \tag{A.8}$$

$$K_{32} = K_{23} \tag{A.9}$$